Kinetics and Catalysis, Vol. 44, No. 2, 2003, pp. 183–197. From Kinetika i Kataliz, Vol. 44, No. 2, 2003, pp. 198–213.

Analysis and Simulation of the Dynamics of a Catalyzed Model Reaction: CO Oxidation on Zeolite Supported Palladium[1, 2]

N. I. Jaeger*, N. V. Peskov, and M. M. Slinko*****

** Institut für Angewandte und Physikalische Chemie, FB 2, Universität Bremen, PF 330440, 28334 Bremen, Germany*

*** Department of Computational Mathematics and Cybernetics, Moscow State University, Moscow, 119899 Russia*

**** Institute of Chemical Physics, Russian Academy of Sciences, ul. Kosygina 4, Moscow, 117334 Russia*

Received September 11, 2002

Abstract—The particle size effect on the oscillatory behavior during CO oxidation over zeolite-supported Pd catalysts is simulated with the help of a deterministic point model and a stochastic mesoscopic model. The point model is developed on the basis of the well-known Sales–Turner–Maple model, which is modified to consider the slow processes of oxidation and reduction of the Pd bulk as well as the effects of the bulk oxidation on the catalyst activity. It is demonstrated that the point model developed can simulate many experimental trends, e.g., the dependence of the catalytic activity and the waveform of the oscillations on the particle size and the pretreatment of the catalyst, as well as the counterclockwise hysteresis, depending on the reaction rate during the cyclic variation of the CO inlet concentration. The higher activity of the smaller particles can be explained by the attainment of a more reduced state of Pd in smaller particles in the course of the reaction. The stochastic model simulates the reaction by a Markovian chain of elementary stages of the reaction. The model variables are the numbers of reagent atoms. Transition probabilities of the stochastic model are chosen in accordance with the rates of the developed point model. It is shown that intrinsic fluctuations and correlations of stochastic variables can significantly change the reaction dynamics on nm-sized particles by extending the oscillatory region in the parameter space.

1. INTRODUCTION

Particle size effects in heterogeneous catalysis affecting the yield and selectivity are well known and have been extensively studied in recent years [1–3]. It was shown experimentally [4] and theoretically [5] that essential differences in the catalytic activity exist between an extended surface and a nanometer-sized cluster. Bridging the materials or structure gap has become one of the major challenges in catalysis research [6]. Aside from strong metal–support interaction in the case of small supported metal particles [7, 8], a number of reasons for the existence of this structure gap have been identified: (i) the complicated structure of the surface of a nm-sized particle, which may include several facets with different crystallographic orientations; (ii) a relatively large fraction of edge and corner atoms; (iii) structural changes of the catalyst particles during the reaction; and (iv) spillover effects, i.e., the migration of adsorbed species between a catalyst particle and its support [4, 5]. In the text below, an additional reason for apparent structure gaps in a heterogeneous catalytic system will be discussed.

Reaction rate oscillations that occur during the oxidation of CO over Pd catalysts have been examined in great detail both under UHV conditions over single crystal surfaces [9] and at an atmospheric pressure over supported catalysts [10–13]. Recently we reported on the effect of the particle size on the dynamic behavior of the oxidation of CO over zeolite supported palladium catalysts [14]. Mathematical modeling demonstrated that this effect might be related to the influence of intrinsic fluctuations in dynamics due to the small number of reactant molecules and surface atoms involved in the case of very small particles in comparison with an extended catalytic surface [15]. With the help of the stochastic model, it was shown that temporal fluctuations of the concentrations of the reactants could drastically change the reaction kinetics on small metal particles with only several hundreds of surface atoms. The stochastic model developed in [15] was based on a mathematical model for CO oxidation over the Pd(110) single crystal face that considered lateral interactions on the surface [16]. However, it is well known that the morphology of a nanometer-sized particle includes various single crystal planes, and the role of edges and corners is essential. The stochastic model developed here is based on a modified model originally proposed by Sales, Turner, and Maple (STM model) to describe the oscillatory behavior of CO oxidation over polycrystalline Pt, Pd, and Ir catalysts [17]. It will be shown here that the characteristic details of the observed effects of the particle size on the dynamic behavior of the reaction

[1] This article was submitted by the author in English.

[2] Paper presented at the 1st International Conference on Highly Organized Catalytic Systems (Chernogolovka, June 24–27, 2003).

0023-1584/03/4402-0183$25.00 © 2003 MAIK "Nauka / Interperiodica"

system can be reproduced by the modification of the STM model.

2. EXPERIMENTAL METHODS AND OBSERVATIONS

The effect of the size of the palladium crystallites on the activity and the dynamic behavior of the catalytic reaction have been studied under shallow bed conditions in a continuous stirred tank reactor (CSTR). The activity and the dynamic behavior of the system have been analyzed under similar experimental conditions for preoxidized catalysts with the same Pd loading, equal to 0.05%, the same surface area of 15.1 cm^2, but with a different size of Pd particles. For catalyst A the size of Pd particles is equal to 10 nm, while for catalyst B the size of Pd particles is equal to 4 nm.

The reaction mixture was fed into the reactor at a flow rate of 150 cm^3/min, corresponding to a linear flow velocity of 1.89 cm/s. The flow rates were controlled by thermal mass flow controllers (HI-TEC, ~1% precision). The outlet CO and CO_2 concentrations were measured by IR analyzer URAS 10E. The details of experimental procedure and catalyst preparation can be found in [14].

The catalytic activity of Pd zeolite catalysts, as well as their dynamic behavior, greatly depends on pretreatment and particle size. Figure 1 depicts the comparison of the catalytic activity of catalysts A and B at 478 K and a 0.5% CO inlet concentration following various pretreatments. The dynamic behavior of catalysts A and B are shown after they were oxidized for 12 h in flowing synthetic air at 633 K (oxidized catalysts) and after treatment with a reactant mixture containing 1% CO in synthetic air at 478 K (reduced catalysts). Figure 1 shows that catalyst B (with 4 nm particles) displays a much higher activity. Moreover, under the chosen experimental conditions, oscillatory behavior can only be observed for preoxidized catalysts, while no oscillations could be detected in the case of the reduced catalyst. Catalyst A (with 10 nm particles) shows under the same experimental conditions a contrasting behavior, i.e., only the reduced catalyst produces oscillations, while the reaction proceeds in a steady state over the preoxidized catalyst. It can also be observed that there is a much smaller difference between the activity of the reduced and the oxidized catalyst B in comparison with catalyst A.

At higher temperatures oscillatory behavior is observed on both catalysts regardless of the nature of the preliminary treatment. The main difference is that only chaotic oscillations could be observed over catalyst B, while in the case of the preoxidized catalyst A, regular oscillations were found to develop in a narrow range of CO inlet concentrations between 0.3 and 0.32 vol % at 503 K. Figure 2 shows for catalyst A sections from an 8 h time series at 503 K and a 0.3% CO inlet concentration. It can be seen how the amplitude, period, and activity increase with time on stream, while the waveform slowly changes as the system spends more time in the high activity state. Initially the preoxidized catalyst A displayed very low activity, and it took some time for the appearance of oscillations. The observed changes are attributed to the establishment of a more reduced state of the catalyst.

Figure 3 shows the dependence of the reaction rate on the CO concentration in the reactor for both catalysts as well as the regions and amplitudes of the reaction rate oscillations. The effective CO concentration in the reactor is used as the abscissa, which under appropriate conditions can oscillate in time. Therefore, the amplitudes of oscillations are shown as slanted bars, which indicate the maximum and minimum of the oscillations. The CO inlet concentration can be derived from the figure by adding the CO_2 concentration in the effluent (ordinate) to the effective CO concentration plotted on the abscissa. Figure 3 demonstrates that the oscillatory region for the catalyst with the smaller Pd particles is larger and the catalytic activity higher.

On both preoxidized catalysts, unusual hysteresis behavior was observed during the variation of the CO inlet concentration. As shown in Fig. 4, the hysteresis in the reaction rate is reversed compared to the usual clockwise hysteresis observed during the CO oxidation on Pt surfaces. This is not a "true" hysteresis, which corresponds to a multiplicity of steady states in the nonlinear system. Its origin is rather connected with the reduction of the preoxidized catalyst at high CO concentration. On the way back, the reaction rate is higher and the region of oscillations is more extended, which is indicative of a reduced catalyst.

Another difference between catalysts A and B can be observed in the transient periods during which a stationary oscillatory state is established over the preoxidized catalysts. A slow increase in the reaction rate with time can be assigned to a slow reduction of the catalyst, and the size of the Pd particles was found to be of significant influence. The transient period is shorter in the case of 4 nm particles compared to 10 nm particles.

3. MATHEMATICAL MODEL

3.1. Point Model for the Reaction on a Catalyst Particle

The oxidation of CO over Pd catalysts has been studied under normal and low pressure conditions [18, 19]. In oxygen excess, the reaction proceeds via the Langmuir–Hinshelwood (LH) mechanism, including the following steps:

$$CO + M \xrightarrow{k_1} MCO, \quad (1a)$$

$$MCO \xrightarrow{k_{-1}} CO + M, \quad (1b)$$

$$O_2 + 2M \xrightarrow{k_2} 2MO, \quad (1c)$$

$$MCO + MO \xrightarrow{k_3} CO_2 + 2M, \quad (1d)$$

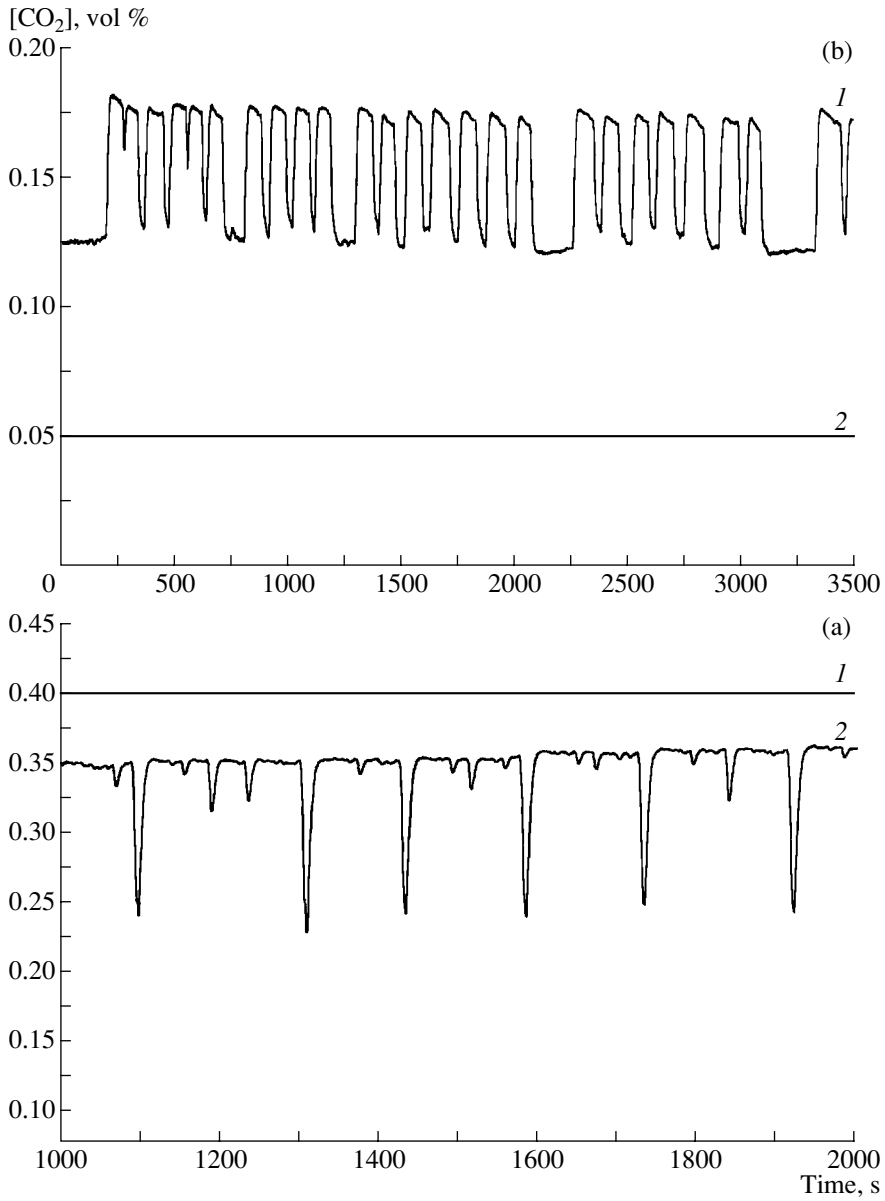

Fig. 1. Comparison of the catalytic activity of catalysts with (a) 4- and (b) 10-nm Pd particles at 478 K and a 0.5% CO inlet concentration following various pretreatment conditions. (*1*) Reduced and (*2*) oxidised catalyst.

where M denotes vacant sites on the metal surface and MCO and MO, adsorbed CO molecules and oxygen atoms, respectively.

The steady-state kinetics follows the first order in CO partial pressure for low CO concentrations (high activity branch) and negative order with respect to CO partial pressure for higher CO concentrations (low activity branch).

The first mathematical model for the simulation of kinetic reaction rate oscillations during the CO oxidation over Pt, Pd, and Ir catalysts was the STM model [17]. Their authors assumed that a slow formation and removal of subsurface oxygen is responsible for the switching of the reaction between the two branches of the LH mechanism [20]. To consider the processes of the oxidation and reduction of the catalyst surface, the following steps were added to the reaction mechanism:

$$MO + M_v \xrightarrow{k_4} M_vO + M, \quad (1e)$$

$$M_vO + MCO \xrightarrow{k_5} M_v + M. \quad (1f)$$

Here M_vO and M_v indicate sites occupied by oxygen atoms and free sites in the subsurface layer.

The experimental results presented in Section 2 show that the dynamic behavior and the properties of the experimentally observed oscillations depend greatly on the pretreatment of the catalyst and on the degree of oxidation of Pd particles embedded into the

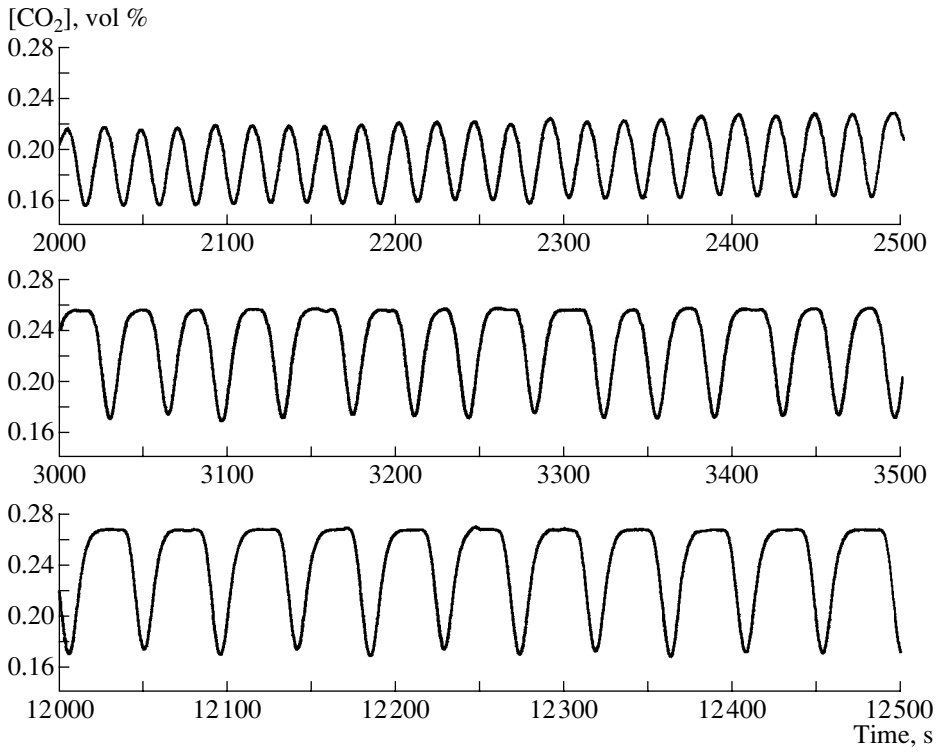

Fig. 2. Evolution of regular oscillations in the case of catalyst A with time on stream at 503 K and 0.3% CO inlet concentration.

zeolite matrix. Recently much experimental evidence was reported concerning the interaction of oxygen with Pd(110) [21] and Pd(111) [22–24] single crystal surfaces and the formation of subsurface oxygen and surface oxide. However, the interaction of oxygen with polycrystalline Pd surfaces, as well as the formation of subsurface and bulk oxide, is still a controversially discussed topic. Meusel *et al.* [25] demonstrated that on small Pd particles of 5–6 nm the formation of subsurface and bulk oxygen is a highly efficient process, which has to be taken into account in kinetic studies.

Therefore, the STM model will be modified to consider the formation of not only the subsurface oxygen but also processes of oxidation and reduction of the bulk of the Pd particle. The additional variable *w*, denoting the degree of the Pd bulk oxidation will be introduced in the model. It may be related with the concentration of the bulk Pd oxide; however, at this stage of mathematical modeling, we are not going to consider the details of the process of Pd oxidation. A mathematical model will be developed based on the following assumptions: (i) subsurface oxygen and bulk oxide have no effect on CO adsorption and desorption; (ii) both subsurface and bulk oxygen prevent O_2 adsorption; i.e., O_2 can adsorb only on a pair of neighboring free Pd surface sites with no bulk oxide and subsurface oxygen underneath; (iii) the surface reaction between chemisorbed CO and O can occur only over nonoxidized Pd; (iv) the limiting oxygen capacity of the subsurface layer is assumed to be $1 - w$; (v) the subsurface oxygen does not diffuse back to the surface but reacts directly with the surface CO.

Thus, if the fraction of the bulk oxide is equal to *w*, the variation of the surface coverage with CO (*x*), the surface coverage with O (*y*), and the concentration of the subsurface oxygen M_vO (*z*) can be described by the system of equations

$$\begin{aligned} \dot{x} &= P_{CO}k_1(1-x-y) - k_{-1}x - k_3(1-w)^2xy - k_5xz, \\ \dot{y} &= P_{O_2}k_2(1-x-y)^2(1-w-z)^2 \\ &\quad - k_3(1-w)^2xy - k_4y(1-w-z), \\ \dot{z} &= k_4y(1-w-z) - k_5xz. \end{aligned} \tag{2}$$

The variables have a physical meaning as long as all of them are nonnegative and $x + y, z \le 1$.

Analysis of the experimental data obtained demonstrates that the activity of the preliminary oxidized catalyst gradually increases with time due to the slow reduction of the Pd particles. This process depends on the size of a Pd particle and the partial pressures of CO and O_2.

The processes of the Pd bulk oxidation and reduction are very complex and intrinsic details of these processes has not yet been clarified. Therefore, in this study to simulate the long-term evolution of the degree

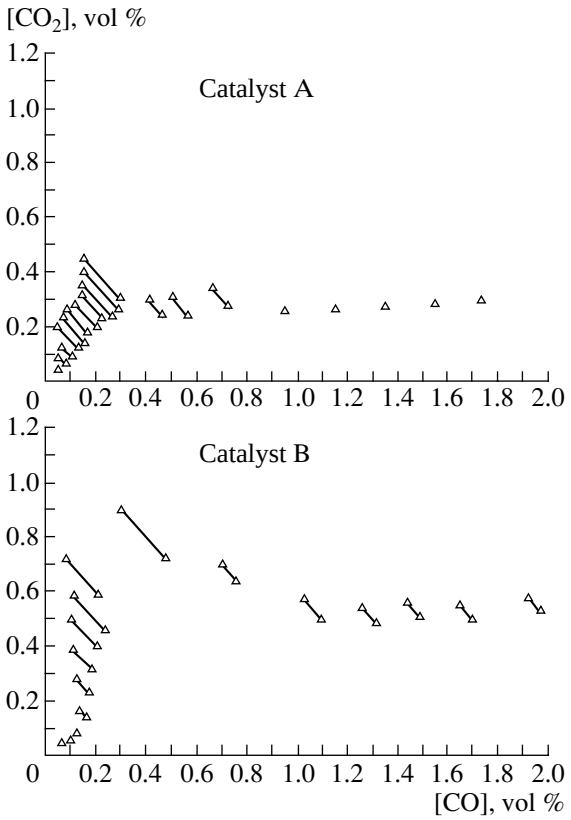

Fig. 3. Reaction rate as a function of CO concentration in the reactor for catalysts A and B at 503 K. The region of kinetic oscillations is indicated by slanted lines, which represent the amplitudes of the oscillations.

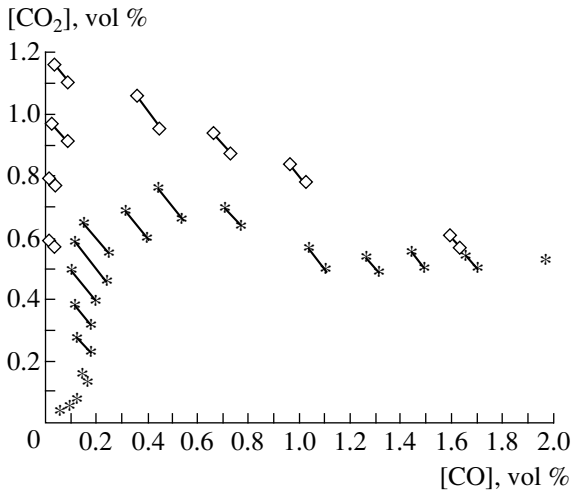

Fig. 4. Counterclockwise hysteresis observed for catalyst B at 503 K during the variation of inlet CO concentration in the feed: (stars) increasing CO concentration, (diamonds) subsequent decrease of the CO concentration.

of bulk Pd oxidation we propose a simple heuristic model expressed by the linear equation:

$$\dot{w} = P_{O_2}k_6(1-w) - k_{-6}P_{CO}sw. \quad (3)$$

This equation assumes that, on a long time scale (compared with the short time scale of reaction rate oscillation), the rate of oxidation is proportional to the oxygen pressure P_{O_2} and the rate of reduction is proportional to the CO partial pressure and to the factor $s = N_s/N$, which denotes the ratio of the number of surface atoms to the total number of atoms in the particle. (The latter is due to the negligible CO diffusion into the bulk of Pd.)

It follows from (3) that, in the course of time, $w(t)$ monotonously approaches the steady state $\bar{w}$ defined by the equation

$$\bar{w} = \frac{1}{1 + p\delta s}, \quad (4)$$

where $p = P_{CO}/P_{O_2}$ and $\delta = k_{-6}/k_6$.

The slow variable w enters the system (2) as a parameter. This makes it possible to study the dynamical behavior of the system as the function of the degree of Pd oxidation.

Parameter s, which was introduced in Eq. (3), allows us to simulate the particle size effect on the dynamic properties of the system. To evaluate the value of s, a small metal particle with an fcc crystal structure was considered. Since a definite shape of the particle is required for the calculation of s, we have chosen the ideal octahedron for the sake of simplicity. The calculations of s were carried out for a lattice constant of Pd crystal of 0.39 nm, depending on the diameter of the octahedron. The results are summarized in the table.

Ratio s of the number of surface atoms to the total number of atoms depending on the diameter d of an octahedral crystal and the fraction of the bulk oxide in the steady state $\bar{w}$

Particle size, nm	N_d, number of atoms on the diameter of the octahedron	N_b, total number of atoms in the octahedron	N_s, number of surface atoms in the octahedron	$s = N_s/N$	$\bar{w}$ at $p = 0.03$ and $\delta = 450$
4	11	891	402	0.451	0.141
10	25	10 425	2306	0.221	0.251
20	51	88 451	10002	0.113	0.396

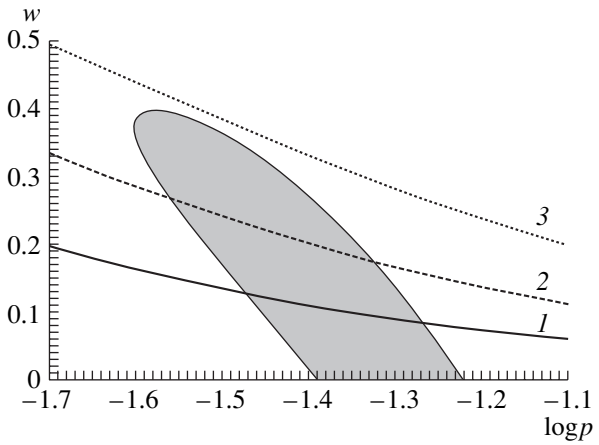

Fig. 5. The region of oscillations produced by model (5) with the values of parameters given in the text. The border of the oscillatory region is the line of Andronov–Hopf bifurcation. The lines $w = \bar{w}(p)$ defined by formula (4) denote the dependence of the concentration of the bulk oxygen on the ratio of partial pressures for (*1*) 4, (*2*) 10, and (*3*) 20 nm-sized particles.

3.2. Certain Qualitative Features of the Point Model Compared with Experimental Data

The chaotic nature of the oscillatory behavior presented in Section 2 and identified in [26] is apparently the result of interaction between many Pd particles via the diffusion of reagents in the pores of zeolite support that cannot be reproduced by our point model, describing the process only on a single Pd particle. In addition, as will be shown below, statistical fluctuations play an important role in the reaction dynamics on the surface of nanometer-sized particles. Therefore, at this stage of mathematical modeling, our goal is to simulate only qualitatively the main features of experimental observations. The values of parameters were taken from the single crystal data [16] and fitted to simulate the reaction rate and the periods of oscillations. The following set of rate constants was used in mathematical modeling:

$$k_1 = 300\ \text{s}^{-1}, \quad k_{-1} = 100\ \text{s}^{-1},$$
$$k_2 = 100\ \text{Torr}^{-1}\ \text{s}^{-1}, \quad k_3 = 4000\ \text{s}^{-1}, \qquad (5)$$
$$k_4 = 0.02\ \text{s}^{-1}, \quad k_5 = 0.019\ \text{s}^{-1}.$$

The characteristic features of oscillations simulated by model (2), (3) with these parameter values are summarized as follows.

1. The region of oscillations. Figure 5 shows the oscillatory region of system (2) in the plane ($\log(p)$, w) obtained with the values of parameters (5). At the border of the region, the oscillations appear via the Andronov–Hopf bifurcation. One can see that with increasing p the oscillations first appear on the oxidized particles at $w = 0.4$ and are absent on the fully reduced catalyst particle. This is in agreement with the experimental observation that at 503 K the catalyst had to be oxidized first in order to obtain reaction rate oscillations. With a further increase in p, the oscillatory region becomes wider and shifts toward the smaller values of w.

Figure 5 also shows the lines $\bar{w}(p)$ of the steady-state value of w depending on p for three particle sizes. The intersection of the line $\bar{w}(p)$ with the shaded region of oscillations indicates the interval of p where the limit cycle solution exists in system (2) for a given particle size. It can be seen from Fig. 5 that oscillatory behavior for 4 nm occurs for a more reduced state of Pd compared to 10 nm particles. This fact is in qualitative agreement with experimental data.

2. Dependence of the properties of reaction rate oscillations on the pretreatment of the catalyst and the degree of catalyst oxidization. One of the common properties of oscillations observed over zeolite-supported Pd catalysts for all sizes of particles is the dependence of the catalytic activity and the waveform of the oscillations on the degree of catalyst oxidation. It was found that in the oscillatory regime the average reaction rate is higher on the more reduced catalyst and the waveform changes from a "spike-up" to a "spike-down" shape during the reduction of the catalyst. Analogous behavior can be simulated by model (2). Figure 6 demonstrates the variation of the oscillations simulated with model (2) for $P_{CO} = 3$ Torr ($\log(p) \approx -1.5$) for various values of the fraction of the bulk oxide w. It can be seen that the reduction of the catalyst, which corresponds to a decrease in w, leads to an increase in the average reaction rate and the transformation of the waveform of the reaction rate oscillations from spike-up to spike-down. An increase in the average reaction rate occurs due to an increase in the rate of step (1d) with decreasing w. The waveform of the oscillations is determined by the duration of the processes of filling and depleting the subsurface layer by oxygen. During the first process, the reaction rate is high, and it is low during the second process. The capacity of the subsurface layer is equal to $1 - w$ in model (2). Therefore, the smaller w, the greater the capacity of the subsurface layer. More time is needed to fill the subsurface layer with oxygen and as a consequence the system remains in the state of high activity for a longer time.

3. Transient processes. Following the admission of the reactants to the preoxidized catalyst, a transient period of time has been observed during which the reaction rate increased slowly without oscillations and only after some time did the oscillations appear. The characteristics of oscillations (waveform and period) slowly changed in time. The time until oscillations appeared was found to be shorter for 4 nm particles compared to 10 nm particles. Analogous behavior can be simulated by model (2), (3). Figure 7 shows the graphs of the reaction rate obtained via simultaneously solving Eqs. (2) and (3) with the initial condition $w = 1$ for 4-nm (Fig. 7a) and 10-nm (Fig. 7b) particles. The values of the parameters of the model were such as

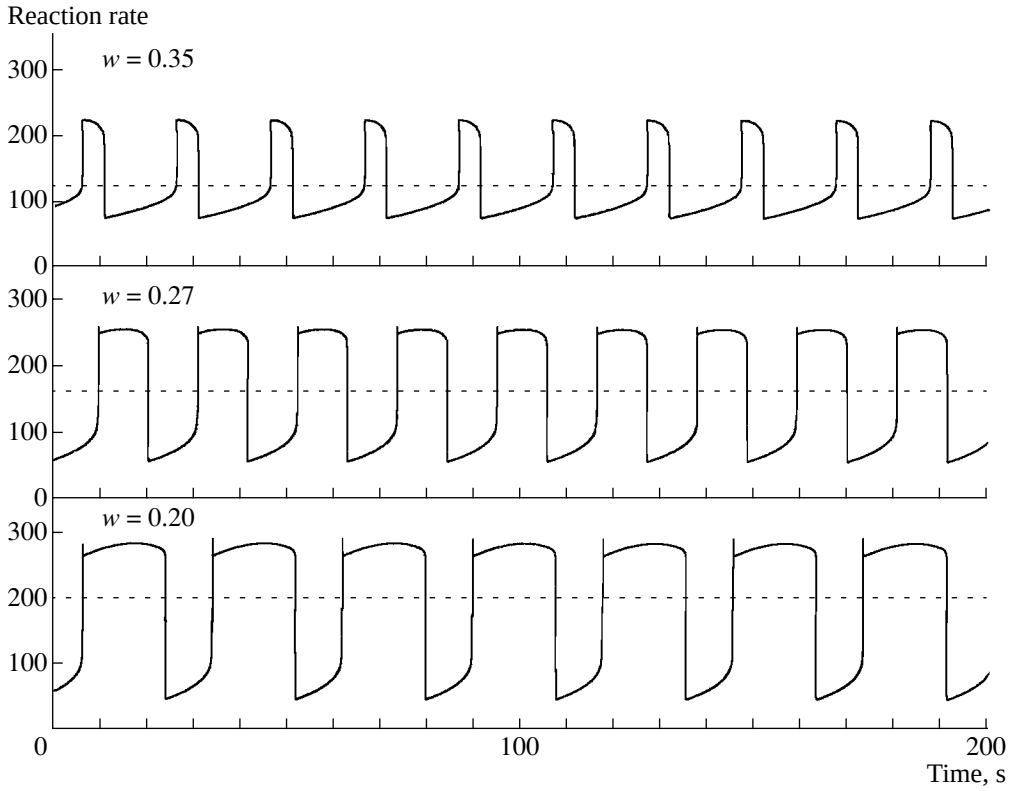

Fig. 6. Time series of the reaction rate obtained from the limit-cycle solution of system (2) for three values of w at P_{CO} = 3 Torr, P_{O_2} = 100 Torr, and k_2 = 100 (Torr s)$^{-1}$. Dotted line in each panel shows the average reaction rate.

determined above, and $k_6 = 10^{-3}$ s^{-1}. The value of the parameter s for a 4-nm particle is about two times larger than for a 10-nm particle. Hence, the rate of the reduction of a 4-nm particle is also two times higher in comparison with a 10-nm particle. As a consequence, the time until the onset of the oscillations is twice as long for a 10-nm particle compared to a 4-nm particle provided the partial pressures of the reactants are the same. Figures 7a and 7b confirm this conclusion. The transformation of the waveform from spike-up to spike-down and the growth of the period of oscillations with time in the case of a 10-nm particle is also in qualitative agreement with experimental data. Regular oscillations were not observed on the catalyst with 4-nm particles; hence, Fig. 7a could not be compared with experimental data. Figure 7c depicts a possible transient regime at P_{CO} = 2.75 Torr ($\log p$ = –1.56) for a 10-nm particle when the steady state $\bar{w}$ lies below the oscillatory region (see Fig. 5). During the reduction process, the value of w passes through the oscillatory region and reaches its steady state $\bar{w}$, where the reaction proceeds in a steady stationary state.

4. Simulations of counterclockwise hysteresis. The results of numerical simulation demonstrate that model (2), (3) can reproduce the counterclockwise hysteresis observed during the change of CO inlet concentration due to the variation of the concentration of the bulk oxide. The example of such hysteresis behavior is shown in Fig. 8 for the catalyst containing 4-nm particles (s = 0.451). The calculations were carried out with a rate of CO partial pressure change equal to 10^{-4} Torr/s and the values for the constants for bulk oxidation and reduction $k_6 = 10^{-7}$ s^{-1} and $k_{-6} = 4.5 \times 10^{-5}$ s^{-1} (δ = 450), respectively. The reaction began on the preoxidized catalyst with the initial condition for w = 1. Figure 8 shows that an increase in P_{CO} leads to a decrease in the concentration of the bulk oxide. On the way back, the concentration of the bulk oxide is lower and, in agreement with experimental data, the activity of the catalyst increases and the region of oscillations is more extended. However, this is not a "true" hysteresis, since for the chosen parameters there is only one steady state in model (2) and the observed apparent hysteresis only appears due to the fact that the slow relaxation of the bulk oxidation does not follow the comparatively fast variation of the CO partial pressure.

3.3. Stochastic Model of the Reaction on a Catalyst Particle

If one supposes that the number of CO and O adsorption centers on the particle surface is equal to the number of surface atoms, this number varies from N_s =

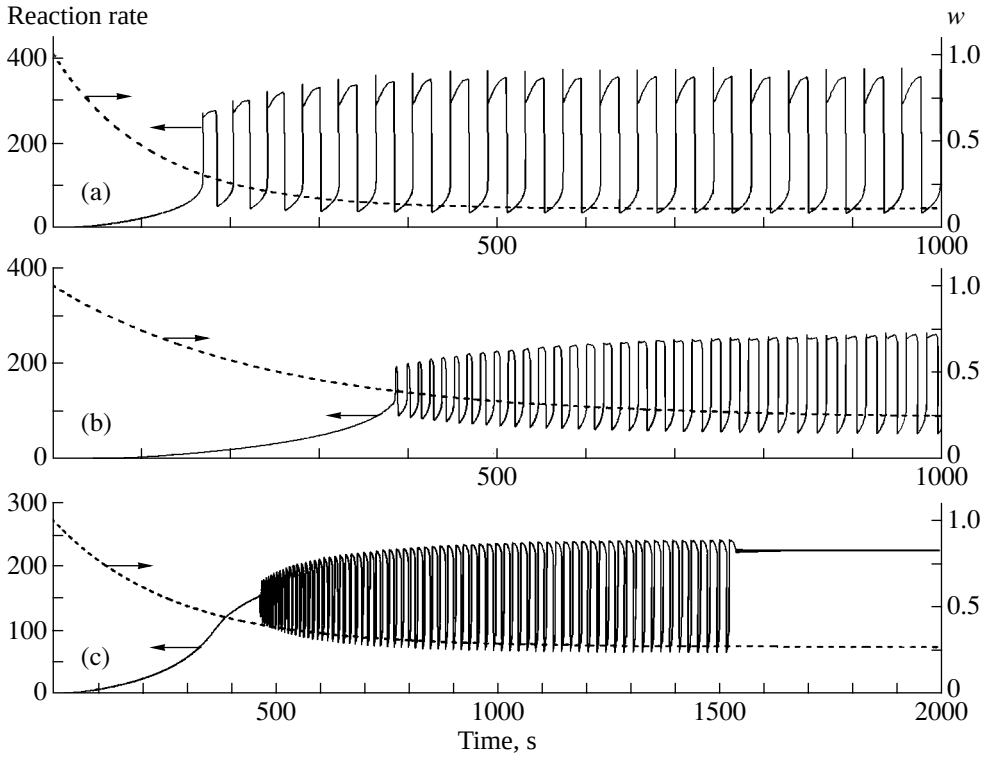

Fig. 7. Time series of the reaction rate R (solid line, left scale) and concentration of the bulk oxide w (dotted line, right scale) obtained by solving the system of equations (2), (3) starting with the initial value of $w = 1$: (a) 4-nm particle, $P_{CO} = 4$ Torr; (b) 10-nm particle, $P_{CO} = 3$ Torr; (c) 10-nm particle, $P_{CO} = 2.75$ Torr.

400 to 10000 while the particle size grows from 4 to 20 nm (table). In the course of the reaction proceeding in the oscillatory regime, the number of adsorbed atoms of each species N_{CO} and N_O, and the number of subsurface oxygen atoms N_{O^*}, can vary in the range between 0 and N_s. At any moment of time, these numbers can be regarded as a set of random values with the unknown probability distribution $\mathbf{P}(N_{CO}, N_O, N_{O^*}; t)$. In this case, Eqs. (2) may be considered as equations for averaged values N_{CO}, N_O, and N_{O^*} divided by N_s. However, these equations can be accurate only in the thermodynamic limit when $N_s \longrightarrow \infty$. At finite and not too large values of N_s, statistical fluctuations of random numbers of atoms can play a significant role and Eqs. (2) may become incorrect. In order to take into account a finite number of atoms participating in the reaction and their statistical fluctuations as well as their mutual correlations, the following Markovian model is proposed.

The model has three discrete variables N_{CO}, N_O, and N_{O^*} that can take nonnegative integer values in the range $[0, N_s]$, and $N_{CO} + N_O \le N_s$, $N_{O^*} \le (1 - w)N_s$. The elementary steps in the reaction scheme correspond to the acceptable transitions in the Markovian model:

CO adsorption: $N_{CO} \longrightarrow N_{CO} + 1$,

CO desorption: $N_{CO} \longrightarrow N_{CO} - 1$,

O_2 adsorption: $N_O \longrightarrow N_O + 2$,

CO + O reaction: $(N_{CO}, N_O) \longrightarrow (N_{CO} - 1, N_O - 1)$,

O $\longrightarrow$ O* transition: $(N_O, N_{O^*}) \longrightarrow (N_O - 1, N_{O^*} + 1)$,

CO + O* reaction: $(N_{CO}, N_{O^*}) \longrightarrow (N_{CO} - 1, N_{O^*} - 1)$.

CO oxidation on the catalyst particle is simulated as a random sequence of acceptable transitions under standard conditions, which implies that multiple transitions are forbidden; any transition can occur at an arbitrary moment of time (Markovian model with continuous time) and is instantaneous. Each transition has its own probability that depends only on the current state of the model (Markovian property).

Instead of transition probability for each event, we define the transition probability per unit time, or the transition rate ν, and then the probability of transition during the time interval Δt will be equal to $\nu\Delta t$. For compatibility with model (2), the transition rates are defined as follows:

$$\nu_1(\mathbf{N}) = k_1 P_{CO}(N_s - N_{CO} - N_O),$$

$$\nu_{-1}(\mathbf{N}) = k_{-1} N_{CO},$$

$$\nu_2(\mathbf{N}) = k_2 P_{O_2}\left(1 - \bar{w} - \frac{N_{O^*}}{N_s}\right)^2 \frac{1}{N_s}$$

$$\times (N_s - N_{CO} - N_O)(N_s - N_{CO} - (N_O + 1)), \qquad (6)$$

$$\nu_3(\mathbf{N}) = k_3(1-\bar{w})^2\frac{N_{CO}N_O}{N_s},$$

$$\nu_4(\mathbf{N}) = k_4\left(1-\bar{w}-\frac{N_{O^*}}{N_s}\right)N_O,$$

$$\nu_5(\mathbf{N}) = k_5\frac{N_{CO}N_{O^*}}{N_s},$$

where $\mathbf{N}$ is the triple $\{N_{CO}, N_O, N_{O^*}\}$, which defines the current state of the model.

Under the conditions described, the time evolution of the state probability distribution $\mathbf{P}(\mathbf{N}; t)$ will be ruled by the master equation

$$\frac{d\mathbf{P}(\mathbf{N}; t)}{dt} = -\sum_{i=-1}^{5}\nu_i(\mathbf{N})\mathbf{P}(\mathbf{N}; t) + \sum_{i=-1}^{5}\nu_i(\mathbf{N}^{(i)})\mathbf{P}(\mathbf{N}^{(i)}; t), \quad (7)$$

where $\mathbf{N}^{(i)}$ denotes the state from which the state $\mathbf{N}$ can be reached via one ith transition. Equation (7) is in fact a large system the dimension of which is equal to the number of all different states of the Markovian model. Although this system could be solved numerically, we will not do this here but instead generate the trajectories of the Markovian process with the help of the Monte Carlo algorithm. Note that with the standard averaging technique the evolution equations for the average values of the model variables can be derived from Eq. (7). For example, the equations for $x(t) = \langle N_{CO}/N_s\rangle$ have the form

$$\dot{x} = k_1P_{CO}(1-x-y) - k_{-1}x - k_3(1-\bar{w})^2xy - k_5xz - \frac{1}{N_s^2}[k_3(1-\bar{w})^2\langle(N_{CO}-\langle N_{CO}\rangle)(N_O-\langle N_O\rangle)\rangle - k_5\langle(N_{CO}-\langle N_{CO}\rangle)(N_{O^*}-\langle N_{O^*}\rangle)\rangle],$$

where the angular brackets $\langle a\rangle$ denote the mathematical expectation of a random value a. Thus, one can see that the equations for the average values of the Markovian model consist of all the terms of the deterministic equations (2) and additional correlation terms. In the limit $N_s \longrightarrow \infty$ the correlation terms are assumed to vanish, but at finite N_s they can play an essential role in the dynamics of the system.

The trajectories of the Markovian process governed by Eq. (7) are generated with the help of one of the Monte Carlo algorithms with continuous time described in [27]. Let t' be the time moment of sequential change in the state of the system. The next time $t'' = t' + \Delta t$ of the state change is determined as follows. The interval Δt between two successive events (the expectation time) is considered to be a random number with the Poisson distribution $\nu(t')\exp(-\nu(t')\tau)$, where

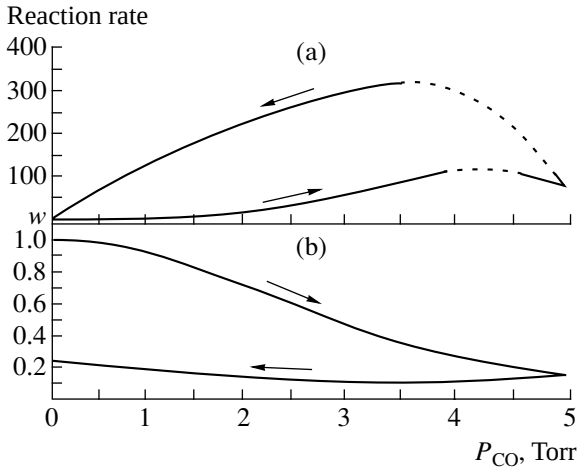

Fig. 8. The dependence of the reaction rate (a) and concentration of the bulk oxide (b) on CO pressure P_{CO}, obtained from the solution of the system (2), (3) for a 4-nm particle. P_{CO} was changing from 0 to 5 Torr and back with the constant rate equal to 0.001 Torr/s. Dotted lines depict the oscillatory region.

$\nu(t') = \nu_1(t') + \nu_{-1}(t') + \nu_2(t') + \nu_3(t') + \nu_4(t') + \nu_{-4}(t')$ is calculated for the state held in the system between t' and t''. Therefore, Δt is defined by the formula

$$\Delta t = -\frac{\ln(\xi_{time})}{\nu(t')}, \quad (8)$$

where ξ_{time} is the random number uniformly distributed in the interval (0, 1). The event, which occurs at time t'', is determined with the help of the other random number ξ_{event} uniformly distributed in the interval $(0, \nu(t'))$. If $\xi_{event} < \nu_1(t')$, then CO adsorption has to occur; if $\nu_1(t') \le \xi_{event} < \nu_1(t') + \nu_{-1}(t')$, then CO desorption has to occur, and so on.

3.4. Results of Stochastic Simulations

In this section we present the results of the simulation of the reaction on 4-, 10-, and 20-nm particles carried out with the help of the stochastic model. The set of parameter values defined for point model (2) was used in the simulations. In addition, it was supposed that $w = \bar{w}$ and slow processes of oxidation and reduction of Pd particle were excluded from the simulation. The results are presented in the form of time series of the reaction rate per one surface site. More exactly, each reading of the reaction rate time series is $R(t_k) = \frac{r_{3,k} + r_{5,k}}{N_s\Delta t}$, where $\Delta t = t_k - t_{k-1} = 0.1$ s, $r_{3,k}$ and $r_{5,k}$ are the numbers of elementary events of reaction CO + O and CO + O*, which happen during the time Δt, respectively. In the subsequent discussion, the distinctive features of the oscillations in the stochastic model will be presented for particles of different sizes.

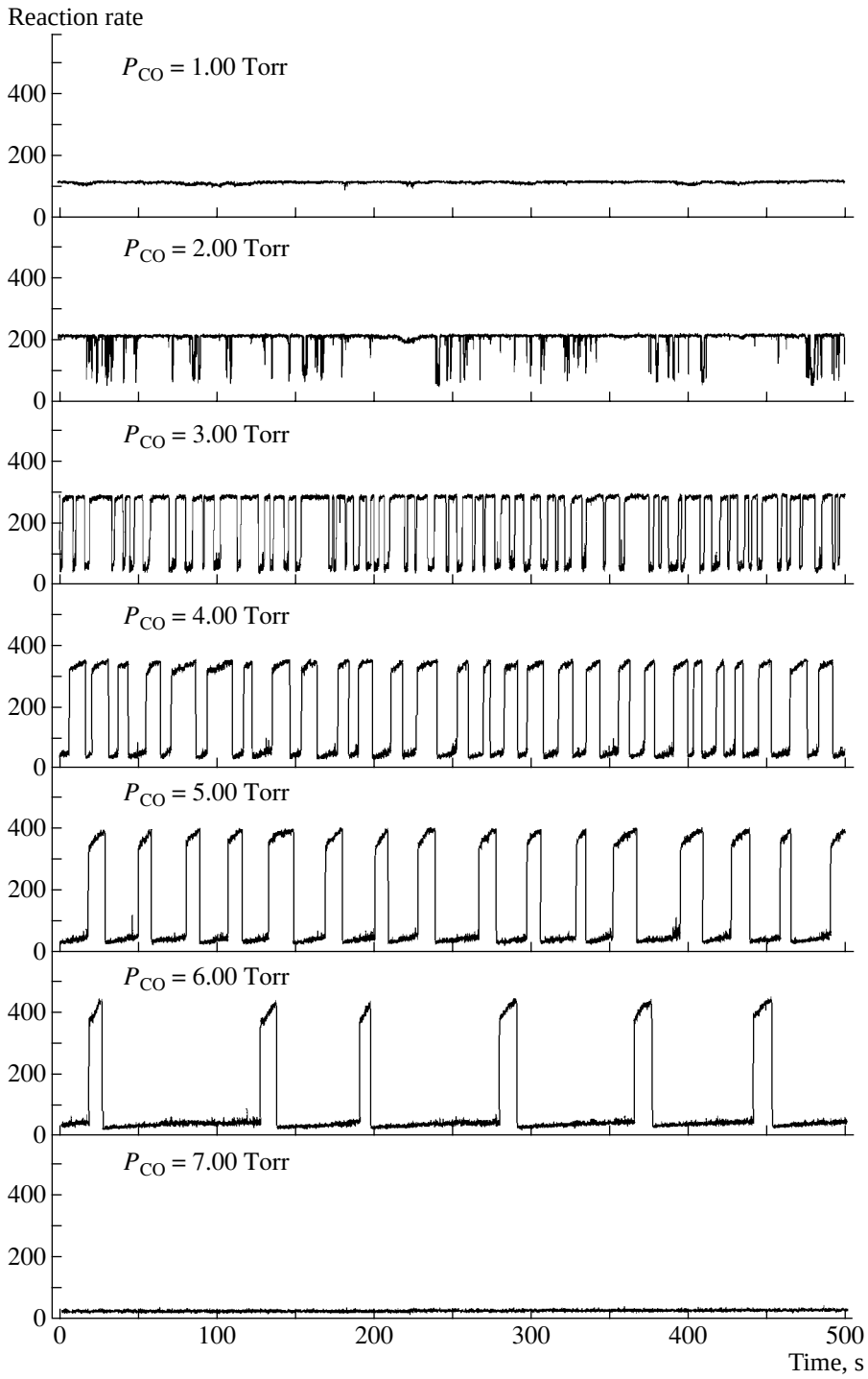

Fig. 9. Time series of the reaction rate produced by the stochastic model at different values of P_{CO} (Torr) in the case of a 4-nm particle.

4-nm particle. The oscillations are observed in the interval $2.00 \le P_{CO} \le 6.00$ Torr, while in the point model the interval of oscillations is $3.37 \le P_{CO} \le 5.41$ Torr. At low P_{CO}, oscillations look like fast and sharp falling spikes in the reaction rate that occur at random moments of time (see Fig. 9). At those moments the reaction rate decreases by about one order of magnitude, i.e., the deviations could not be regarded as statistical fluctuations. With increasing P_{CO}, the spikes gradually become wider. At high P_{CO} the reaction proceeds mostly with a low rate interrupted by large random bursts. The oscillations look like a sequence of transitions between two basic states in the phase space of the model, which happen at random moments of time. At all values of P_{CO} where oscillations exist, they are highly aperiodic and this fact might be a reason why

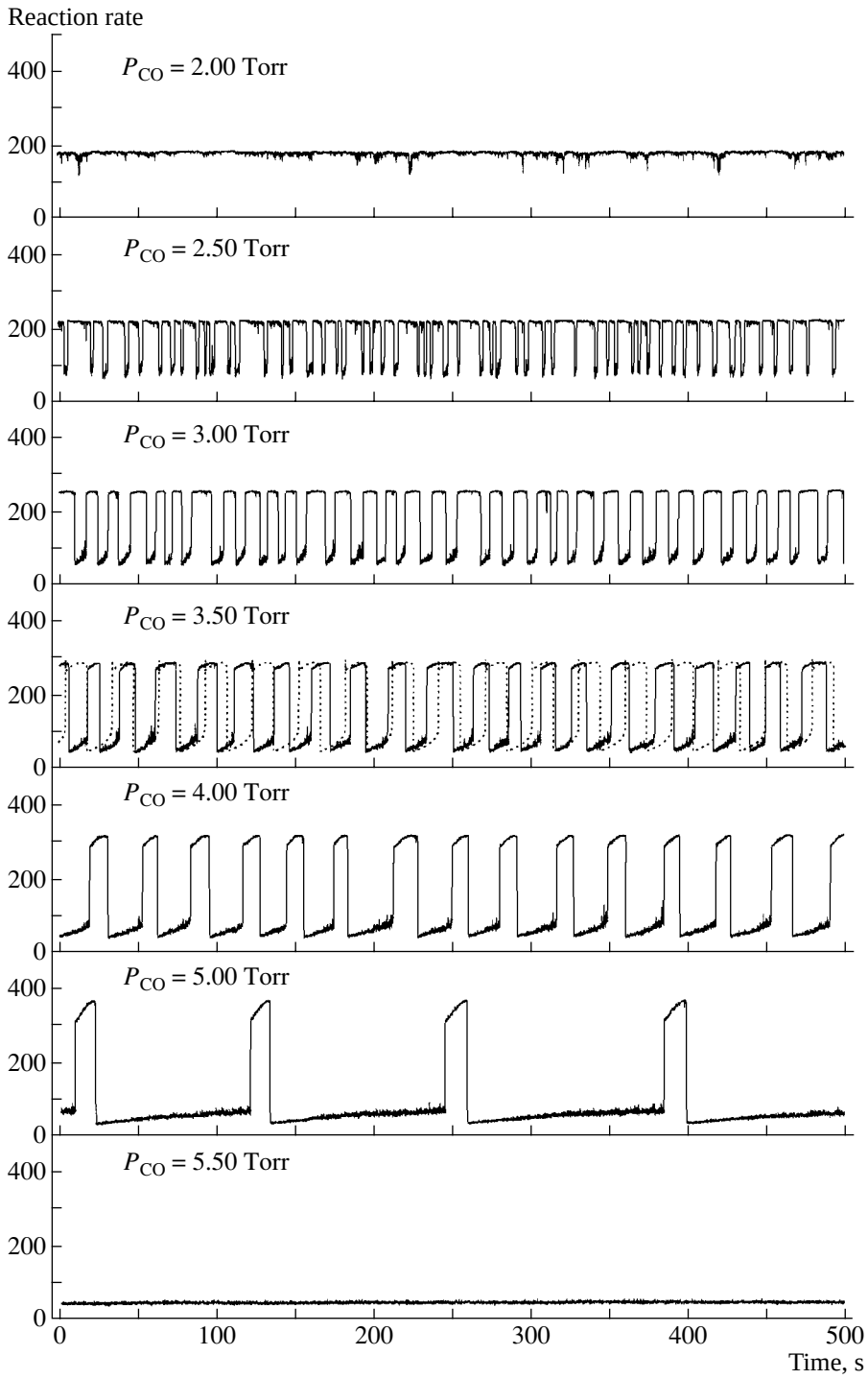

Fig. 10. Time series of the reaction rate produced by the stochastic model for different values of P_{CO} (Torr) for the case of a 10-nm particle. The dotted line in the panel for P_{CO} = 3.5 shows the values of the reaction rate produced by the deterministic model under the same conditions.

regular oscillations have not been observed on catalysts containing 4-nm particles.

10-nm particle. Oscillations are observed in the interval of about $2.50 \le P_{CO} \le 5.00$ Torr, while in the point model the oscillatory region is $2.76 \le P_{CO} \le 4.73$ Torr. This CO pressure interval is slightly shorter than in the case of the 4-nm particle. The shrinking of the interval of the CO pressure where oscillations occur is in agreement with the experimental data. While the pressure P_{CO} increases through the oscillatory region, the shape of the oscillation changes similarly to the previous case

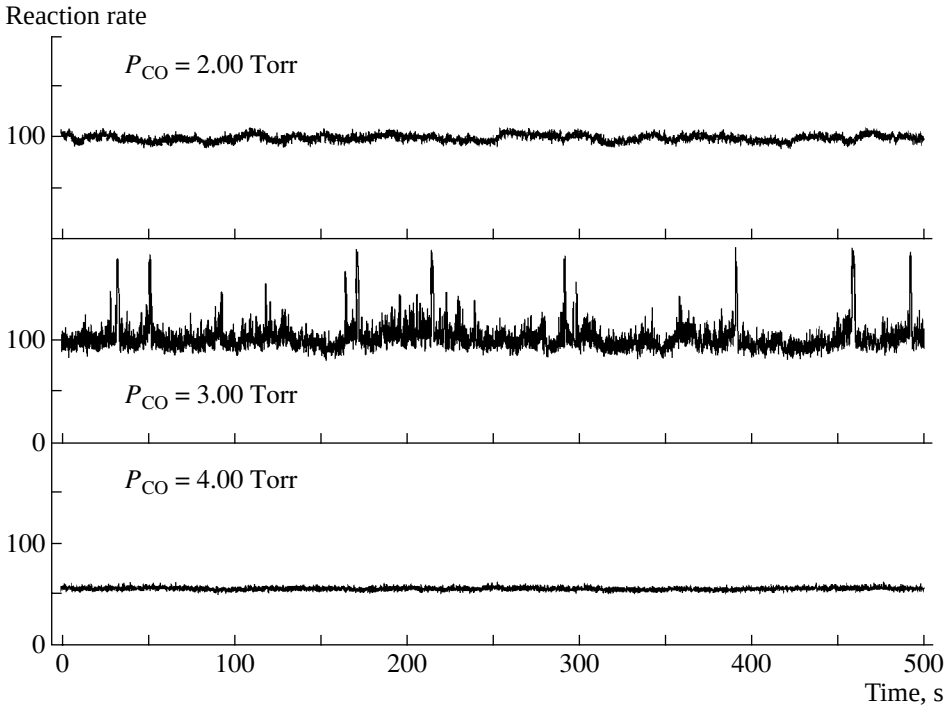

Fig. 11. Time series of the reaction rate produced by the stochastic model for different values of P_{CO} (Torr) in the case of a 20-nm particle.

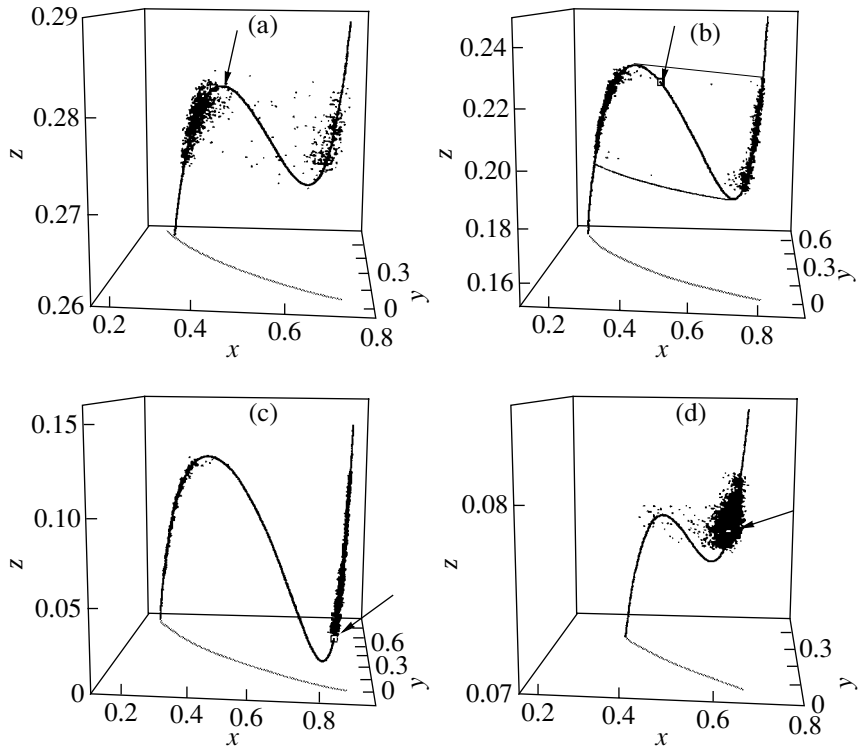

Fig. 12. 3D images of phase trajectories produced by the stochastic model and nullcline *S*: $x = y = 0$ of the deterministic model (2). The small white square indicates the position of the stationary solution of the model (2). (a) 10 nm, P_{CO} = 2.5 Torr; (b) 10 nm, P_{CO} = 3.5 Torr. The thin solid line represents the limit cycle generated by model (4); (c) 10 nm, P_{CO} = 5 Torr; (d) 20 nm, P_{CO} = 3 Torr.

of the 4-nm particle, but the oscillations reveal a more regular character and their amplitude is smaller (see Fig. 10). Such oscillations on separated particles could probably be synchronized via the gas phase diffusion yielding regular oscillations of the global reaction rate. For comparison purposes, the reaction rate oscillations obtained from the point model for P_{CO} = 3.5 Torr are shown as a dotted line in Fig. 10. It can be seen that the stochastic and the deterministic oscillations have similar forms, but the former have a shorter (average) period than the latter. During the time interval presented there are about 20 stochastic cycles and about 16 deterministic cycles.

20-nm particle. The phase diagram in Fig. 5 shows that there are no self-sustained oscillations in the point model for 20-nm particle. However, it can be expected that, in the stochastic model, oscillations would be possible for those values of P_{CO} where the curve $\bar{w}(p)$ passes through the vicinity of the border of the oscillatory region. Figure 11 confirms this expectation. Indeed, in the case of P_{CO} = 3 Torr, stochastic oscillations can be observed near the oscillatory region. These oscillations have the form of occasional short bursts. During such a burst, the reaction rate increases by a factor of 2.

Figure 12 clarifies the mechanism of stochastic oscillations. It depicts 3D images of the phase trajectory of the stochastic model together with the line of slow motion **S**: ($\dot{x} = 0$, $\dot{y} = 0$) of the system (2) (thick solid line) and the stationary solution of system (2) shown in the figure by the small white square lying in the line **S**. The line **S** is, in essence, the line of the stationary states of the LH reaction depending on the parameter z. The part of **S** lying between the extremes is unstable (repelling) and the two outer branches are stable (attracting). In Fig. 12, the left attractive branch of **S** is the high activity branch, while the right one is the low-activity branch. Black points, which indicate the position of the current state of the stochastic model, cloud mostly around the attractive branches of **S**.

Figures 12a–12c are related to a 10-nm particle. In the case of P_{CO} = 2.5 Torr (Fig. 12a), the stationary solution to system (2) lies on the high-activity branch of **S**, and system (2) has no limit cycle solutions. However, the state of the stochastic model cannot stay in the vicinity of the stationary solution of the deterministic model all the time. Statistical fluctuations may occasionally move it into the domain of attraction of the low-activity branch and, to go back, the phase point has to go a long way to the opposite branch of **S**, passing along this branch in the direction of the extreme and falling back to the first branch. The high-activity branch containing the stationary solution to system (2) is more attractive than the opposite branch; hence, the phase point of the stochastic model spends more time near the high activity branch, and the oscillations have a spike-down shape.

In the case of P_{CO} = 3.5 Torr (Fig. 12b), system (2) has a limit cycle solution shown by the thin solid line. However, due to the presence of fluctuations, the phase point of the stochastic model does not follow exactly the deterministic trajectory and can leave the limit cycle before its breakdown point. Therefore, the average period of stochastic oscillations is shorter than the period of the limit cycle in the deterministic model.

In the case of P_{CO} = 5 Torr, the stationary solution to system (2) lies on the low-activity branch of **S**, and as in the case shown in Fig. 12a, system (2) has no limit cycle solutions. Now the phase point of the stochastic model spends more time near the low-activity branch, and because this branch is more stable than the high activity one, the oscillation has a spike-up form with a long average period.

Fig. 12d illustrates the oscillations in the stochastic model of the reaction on a 20-nm particle at P_{CO} = 3 Torr. Here the stationary solution to (2) lies on the low-activity branch of **S** and sufficiently close to one of its extremes. In such a situation, the fluctuations are able to throw the phase state of the stochastic model to the other branch of **S**.

4. DISCUSSION AND CONCLUSIONS

This paper presents two models designed to simulate the particle size effect that has been observed during the study of the dynamic behavior of CO oxidation over zeolite-supported Pd catalysts. One of the most interesting problems was to understand the possible reason for the experimental observation that catalyst B with 4-nm particles produced only chaotic oscillations, while catalyst A with 10-nm Pd particles can generate regular oscillations under appropriate experimental conditions. In Section 3.1 a new point deterministic model was developed to simulate the reaction rate oscillations observed during the CO oxidation depending on the size of Pd particles. Many experimental trends could be modeled successfully, e.g., the dependence of the catalytic activity and the waveform of oscillations on the particle size and the pretreatment of the catalyst, as well as the counterclockwise hysteresis in the dependence of the reaction rate during the cyclic variation of the CO inlet concentration. The higher activity of the smaller particles can be explained by the attainment of a more reduced state of the Pd in smaller particles in the course of the reaction. Such a situation occurs because the process of the bulk reduction of Pd was assumed to be proportional to the parameter s, which indicates the ratio of the number of surface atoms to the total number of atoms in the particle. In this case, the smaller particles reach a less oxidized state during the reaction, resulting in a higher activity.

The stochastic model developed in this work reveals a significant role of internal fluctuations during heterogeneous catalytic reactions on nanometer-sized supported metal particles. The results of simulations with

the stochastic model shown in Figs. 9–11 demonstrate the large difference in the oscillatory behavior of the reaction rate for particles of various sizes. For the same parameters and experimental conditions, the region of oscillations for 4-nm particles is much larger than for 20-nm particles due to the much larger effect of internal fluctuations on the small particles. The comparison of oscillations for 4- and 10-nm particles demonstrates that 4-nm particles produce more complex and irregular oscillations in a larger region of CO partial pressures compared to 10-nm particles in accordance with experimental data. The cause of the drastic increase in the oscillatory region for the catalyst with the smallest particles is associated with the presence of noise-induced oscillations, i.e., oscillations that can be produced only by the stochastic model and that are absent in the deterministic limit.

Only recently has attention been paid to the possibilities of noise-induced oscillations in heterogeneous catalytic systems [28–30]. The role of the external noise has been analyzed by Hou *et al.* [28, 29]. The models that were developed for the simulation of kinetic oscillations in the NO + CO reaction over Pt(100) [28] and $CO + O_2$ reaction [29] were subjected to external parametric noise. It was demonstrated that, in both reactions, noise-induced oscillations in the absence of deterministic oscillations could arise near the supercritical Andronov–Hopf bifurcation.

The role of internal fluctuations in the dynamic behavior of CO oxidation over low-index single crystal surfaces has recently been studied by Reichert *et al.* [30]. The stochastic model was developed for CO oxidation on low-index platinum single crystal surfaces. It was demonstrated that internal fluctuations became essential only for very small surface cells, such as field emitter tips with a 20×200 Å area. For larger single crystal surfaces, the internal fluctuations are averaged out and do not affect the dynamic behavior of the system. The present study demonstrates that noise-induced oscillations can arise in the case of particle sizes of 20 nm and smaller.

A similar problem, i.e., how the oscillations can be modified with a decrease in the active catalyst surface, was analyzed by Zhdanov [31]. The author carried out Monte Carlo analysis of the microlevel model, based on an STM oscillatory mechanism, varying the lattice size from 50×50 to 3×3. It was demonstrated that more or less regular oscillations can be observed down to 15×15. The conclusion was drawn that in principle one can employ the mean-field approximation even for a very small (~5 nm) catalyst particle. However, the analysis of mesoscopic level model (7) based on the modified STM model to simulate, in particular, the particle size effect demonstrates that the problem may arise even for larger particles.

The particle size effect is usually explained by the presence of such factors as reactant supply via the support, particle–support interaction or variation of the catalytic activity of the particle with its size due to adsorbate-induced reshaping [32–34]. The present study, together with our previous paper [15], suggests another origin of the particle size effect, namely the presence of internal fluctuations and the variation of the degree of oxidation of a noble metal particle during the reaction. While the second cause can be recognized during the study of the steady-state behavior, the particle size effect due to the presence of internal fluctuations can only be identified during the study of oscillatory behavior.

Finally, we note that the stochastic model developed in this paper is only able to simulate the oscillatory behavior on one catalyst particle. The mathematical modeling of the collective behavior of an array consisting of many such particles will be the subject of future work.

ACKNOWLEDGMENTS

The authors acknowledge financial support from the Russian Foundation for Basic Research (grant no. 00-03-32125) and INTAS (grant no. 99-1882).

REFERENCES

1. Che, M. and Benett, C.O., *Adv. Catal.*, 1989, vol. 36, p. 55.
2. Bond, G.C., *Chem. Soc. Rev.*, 1991, vol. 20, p. 441.
3. Bukhtiyarov, V.I. and Slinko, M.G., *Rus. Chem. Rev.*, 2001, vol. 70, p. 167.
4. Henry, C.R., *Appl. Surf. Sci*., 2000, vol. 164, p. 252.
5. Zhdanov, V.P. and Kasemo, B., *Surf. Sci. Rep*., 2000, vol. 39, p. 25.
6. Freund, H.-J., Bäumer, M., and Kuhlenbeck, K., *Ad. Catal.*, 2000, vol. 45, p. 333.
7. Tauster, S.J., Funk, S.C., and Garten, R.L., *J. Am. Chem. Soc*., 1978, vol. 100, p. 170.
8. Hippe, C., Lamber, R., Schulz-Ekloff, G., and Schubert, U., *Catal. Lett.*, 1997, vol. 43, p. 195.
9. Basset, M.R. and Imbihl, R., *J. Chem. Phys*., 1990, vol. 93, p. 811.
10. Böcker, D. and Wicke, E., *Ber. Bunsen-Ges. Phys. Chem*., 1985, vol. 89, p. 629.
11. Jaeger, N.I., Möller, K., and Plath P.J., *J. Chem. Soc., Faraday Trans. I.*, 1986, vol. 82, p. 3315.
12. Slinko, M.M., Jaeger, N.I., and Svensson, P., *J. Catal.*, 1989, vol. 118, p. 349.
13. Jaeger, N.I., Liauw, M.A., and Plath, P.J., *J. Chem. Phys*., 1996, vol. 104, p. 6375.
14. Slin'ko, M.M., Ukharskii, A.A., Peskov, N.V., and Jaeger, N.I.,*Catal. Today.*, 2001, vol. 70, p. 341.
15. Peskov, N.V., Slinko, M.M., and Jaeger, N.I., *J. Chem. Phys*., 2002, vol. 116, p. 2098.
16. Hartmann, N., Krischer, K., and Imbihl, R., *J. Chem. Phys.*, 1994, vol. 101, p. 6717.
17. Sales, B.C., Turner, J.E., and Maple, M.B., *Surf. Sci*., 1982, vol. 114, p. 381.
18. Turner, J.E., Sales, B.C., and Maple, M.B., *Surf. Sci.*, 1981, vol. 109, p. 591.

19. Engel, T. and Ertl, G., *J. Chem. Phys*., 1978, vol. 69, p. 1267.
20. Turner, J.E., Sales, B.C., and Maple, M.B., *Surf. Sci.*, 1981, vol. 103, p. 54.
21. Bondzie, V.A., Kleban, P.H., and Dwyer, D.J., *Surf. Sci.*, 1996, vol. 247, p. 319.
22. Voogt, E.H., Mens, A.J.M., Gijzeman, O.L.J., and Genus, J.W., *Surf. Sci.*, 1997, vol. 373, p. 210.
23. Zheng, G. and Altman, E.I., *Surf. Sci*., 2000, vol. 462, p. 151.
24. Leisenberger, F.P., Koller, G., Sock, M., *et al.*, *Surf. Sci*., 2000, vol. 445, p. 380.
25. Meusel, I., Hoffmann, J., Hartmann, J., *et al*., *Catal. Lett.*, 2001, vol. 71, p. 5.
26. Slin'ko, M.M., Ukharskii, A.A., Peskov, N.V., and Jaeger, N.I., *Faraday Disc.*, 2001, vol. 120, p. 179.
27. Gillespie, D.T., *Physica A*, 1992, vol. 188, p. 404.
28. Hou, Z. and Xin, H., *Phys. Rev. E*, 1999, vol. 60, p. 6329.
29. Hou, Z., Yang, L., and Xin, H.J., *Chem. Phys*., 1999, vol. 111, p. 1592.
30. Reichert, Ch., Starke, J., and Eiswirth, M., *J. Chem. Phys*., 2001, vol. 115, p. 4829.
31. Zhdanov, V.P., *Catal. Lett*., 2000, vol. 69, p. 21.
32. Gunter, P.L.J., Niemantsverdriet, J.W., Ribeiro, F.H., and Somorjai, G.A., *Catal. Rev. Sci. Eng*., 1977, vol. 39, p. 77.
33. Conner, W.C. and Falconer, J.L., *Chem. Rev.*, 1995, vol. 95, p. 759.
34. Zhdanov, V.P. and Kasemo, B., *Surf. Sci*., 1998, vol. 405, p. 27.